Coal Gasification in a Transport Reactor

Lawrence J. Shadle*

U.S. Department of Energy, National Energy Technology Laboratory, P.O. Box 880, Morgantown, West Virginia 26507-0880

Esmail R. Monazam

REM Engineering Services, 3566 Collins Ferry Road, Morgantown, West Virginia 26505

Michael L. Swanson

Energy & Environmental Research Center, University of North Dakota, Grand Forks, North Dakota 58202-9018

An advanced transport reactor gasifier was operated using three different coals: Illinois #6 bituminous, Wyodak Powder River Basin subbituminous, and a Sufco Utah bituminous coals. A steady-state model was developed to evaluate the relative contributions of coal combustion and gasification of coal/char in this high-throughput reactor. The tests employed in-bed calcium-based sorbent for sulfur capture. The model was based on elemental mass and energy balances and assumed instantaneous devolatilization and combustion and kinetically limited gasification reactions in a continuously stirred tank reactor. The experimental results on the reaction of these three coals were compared with model predictions. The simulated results compared favorably with the experimental results (e.g., gas composition, carbon conversion, and reactor temperature). The bituminous coal data were accurately simulated as substoichiometric combustion processes. The more reactive subbituminous coal exhibited significant gasification conversion over the operating conditions tested. The subbituminous coal was found to react 20 times faster than reported from laboratory kinetic studies. The model was used to predict the performance of the gasifier, including the carbon conversion, sulfur capture, and composition and flow rate of product gas, based on operating conditions and input streams. Sensitivity studies on the coal feed rate, steam/coal ratio, heat loss, pressure, gas velocity, and coal reactivity were conducted. These simulations were used to compare the response of coals gasified to those combusted substoichiometrically, to evaluate the optimum operating conditions and to predict the performance in larger-scale units with less heat loss.

Introduction

Advanced power systems employ coal gasification to enhance power production efficiency and environmental performance. The pressurized transport reactor was proposed to be an advanced gasification concept.[1] This reactor is a high-velocity, pressurized adaptation of the circulating-fluid-bed process commonly used for combustors in commercial waste fuel boilers. The elevated pressure and high gas velocities provide the potential for a high coal flux or throughput per cross-sectional unit area. In addition, the plug-flow nature of this technology is designed to physically separate char combustion at the base of the mixing zone from coal gasification above to enhance gas product quality. Unfortunately, because of the height required in a transport reactor process, even a small-scale unit is quite large. To test this concept the Department of Energy funded the Transport Reactor Development Unit (TRDU) that was built at the University of North Dakota.

The transport reactor operates in a unique time−temperature regime for a coal gasifier. Fixed-bed and fluid-bed gasifiers use tens of minutes or longer and low exit temperatures (250−500 °C for fixed-bed; 800−1100 °C for fluidized-bed) to convert the char to fuel gas. Entrained-flow gasifiers use high temperatures (1350−1550 °C) and gasify coals in 2−3 s. The transport gasifier operates with the same exit temperatures as fluid-bed reactors but with short solids residence times, typically ranging from 5 to 30 s using small particles (100−300 μm in diameter). No data are available on coal char gasification over this time period without cooling and reheating of the char.

Coal conversion in a gasifier is a combination of devolatilization and gas−solid reaction. Pyrolysis and combustion studies demonstrate that both of these processes are rapid and can be considered complete for even the most unreactive coals within the time period and operating temperatures available in circulating fluid beds (CFBs) when one considers the particles sizes of interest in transport reactors.[2−4] Gasification rates, however, depend on the feedstock, catalytic constituents, and heat-treatment conditions. The degree of coalification is known to influence the gasification rates.[5,6] Low-rank coals have greater reactivity and greater variability. High temperature, long soak times at elevated temperatures, and slow heating rates during heat-up and pyrolysis all deactivate the coal char toward gasification processes.[5,7,8] Loss of volatile yield and char

* Author to whom correspondence should be addressed. E-mail: Lawrence.Shadle@NETL.DOE.Gov. Fax: (304)-285-4403. Phone: (304)-285-4647.

10.1021/ie001113u
Published on Web 05/25/2001

deactivation during pyrolysis are thought to result from secondary cracking reactions of tars and volatiles.[2] For low-rank coals with ion-exchangeable cations, char deactivation has been found to result from loss of dispersion of the catalytic species.[9] It is expected that a process operating at low temperatures, high heating rates, and short residence times would result in relatively high reactivities.

The goal of this research was to evaluate the test data and performance of the transport reactor as an advanced gasifier. It is the purpose of this study to identify future directions for transport reactor enhancements and to optimize operating conditions and reactor performance. In pursuit of these objectives, a computer model for gasification and combustion in a circulating fluid bed was developed, validated, and enhanced to provide a predictive tool.

As research and development continues on circulating-fluid-bed reactors, a mathematical model is necessary to gain insight into the influence of design variables and feed materials on the reactor performance. A mathematical model promotes understanding of scale-up, design, operation, and control of any process; circulating-fluid-bed combustion and gasification is no exception. Modeling of this process requires a knowledge of the hydrodynamics and chemical reactions that take place in a circulating-fluid-bed reactor. Few papers are available in the literature on the circulating-fluid-bed combustor modeling, and none on circulating fluidized beds (CFBs) with combined combustion and gasification. Therefore, any mathematical modeling developed for this new process must be verified experimentally before it can be implemented in practice.

Weiss et al.[10] presented a mathematical model for a circulating-fluid-bed combustor using a continuous-stirred-tank reactor (CSTR) for both gas and solids in the riser. Their model uses the kinetics of bubbling-fluidized-bed combustors developed by Rajan and Wen.[11] Arena et al.[12] presented a model of CFB combustion of char in which the riser was divided into three blocks: the dense zone at the bottom (block 1), the dilute zone at the top (block 3), and an intermediate zone where the solids concentration decreased following a sigmoidal curve (block 2). They also assumed plug flow of the gas and complete mixing of the solids for all three riser blocks. Adánes et al.[13] modeled the carbon combustion efficiency of CFB combustion using a shrinking particle model with mixed control by chemical reaction and gas film diffusion. The model considered the bed as two regions: a dense region at the bottom with a constant voidage of 0.82 and a dilute region in the upper part in which the solids fraction decreased exponentially as the bed height increased.

Combustion in CFBs was successfully modeled using both plug-flow and CSTR approaches. In the present work, a mathematical model of coal gasification was developed to described the steady-state operation of a circulating fluid bed with an in-bed calcium-based sorbent for sulfur capture. The model has adopted the CSTR approach. The kinetics of char gasification and CaO desufurization were built into a solids residence time distribution based on the hydrodynamics of a circulating fluid bed.

Theory

In a circulating-fluid-bed reactor, fresh solids (coal and sorbent) and hot circulating char are fed into a fast moving gaseous (air/oxygen and steam) medium, thereby transporting the solids. As the solids travel upward, the coal/char reacts with oxygen and steam to produce CO_2, CO, H_2, CH_4, and other hydrocarbons. The principal mechanisms involved in coal combustion and gasification in a CFB reactor have not been reported in the literature. However, numerous models are available for the gasification of coal in a fluid-bed reactor, and we have chosen to apply these kinetic models to CFB reactors. Therefore, in this study, fluid-bed kinetics was adopted to describe the gasification kinetics in the transport reactor. This model assumes that the reaction takes place only in the riser of the transport reactor. Char does not react in any other sections of the transport reactor because these sections are purged and operated under inert conditions. The model solves for the steady-state solution using the Eulerian frame of reference; thus, one does not need to consider the number of times that a given particle happens to be cycled through the riser. Instead, the nature of the solids entering and leaving the riser, the inventory, and average residence times must be specified and must be internally consistent. The other assumptions concerning the riser hydrodynamics, devolatization, combustion, and gasification are discussed below.

Hydrodynamics. The riser section of a CFB usually operates in the fast-fluidized regime. Experimental evidence from Yerushalmi and Cankurt[14] suggests that a circulating-bed riser has two regions: a lower dense region of uniform voidage and an upper dilute region. The axial voidage profile in the dense-phase transport region is assumed to be constant, and its average voidage, $\bar{\epsilon}_{\text{dense}}$, is obtained using the King[15] correlation

$$\bar{\epsilon}_{\text{dense}} = \frac{U_g + 1}{U_g + 2} \tag{1}$$

The axial voidage profile in the dilute region is analyzed with an exponential model as[16]

$$\epsilon_{\text{dil}}(h) = \epsilon^* + (\bar{\epsilon}_{\text{dense}} - \epsilon^*)\mathrm{e}^{-ah} \tag{2}$$

where ϵ^* is the saturated voidage above transport disengaging height (TDH) where the voidage is constant. The value of ϵ^* is calculated from[17]

$$\epsilon^* = \left[1 + \frac{\lambda(U_g - U_t)^2}{2gD_r}\right]^{-1/4.7} \tag{3}$$

where λ depends on system parameters.[17] The decay constant, a, is an important parameter, and its value depends on the gas velocity and particle properties.[16]

The height of the dilute-phase transport region is estimated by

$$H_{\text{dil}} = \frac{1}{a}\ln\left(\frac{\epsilon^* - \bar{\epsilon}_{\text{dense}}}{\epsilon^* - \epsilon_e}\right) \tag{4}$$

where ϵ_e is the voidage at the riser exit, which was estimated by assuming that the slip velocity at the exit is equal to terminal velocity[16]

$$\epsilon_e = 1 - \frac{G_s}{\rho_s(U_g - U_t)} \tag{5}$$

The average voidage in the dilute-phase transport

region, $\bar{\epsilon}_{dil}$, is expressed as[16]

$$\bar{\epsilon}_{dil} = \epsilon^* + \frac{\bar{\epsilon}_{dense} - \epsilon_e}{aH_{dil}} \quad (6)$$

The height of the dense-phase transport region is estimated as

$$H_{dense} = L_r - H_{dil} \quad (7)$$

where L_r is the total height of the riser.

The solids inventories in the dense-phase and dilute-phase transport regions are approximated as

$$I_{dense} = \rho_s(1 - \bar{\epsilon}_{dense})A_r H_{dense} \quad (8)$$

and

$$I_{dil} = \rho_s(1 - \bar{\epsilon}_{dil})A_r H_{dil} \quad (9)$$

respectively. The total solids inventory in the riser is obtained by summing the dense and dilute regions of the riser

$$I_r = I_{dense} + I_{dil} \quad (10)$$

Devolatilization and Combustion. The devolatization kinetics is assumed to be instantaneous and to produce CO, CO_2, H_2, H_2O, and CH_4 as product gases. The carbon conversion due to devolatization incorporates a specified value for the number of moles of CH_4 produced per mole of carbon fed and is based on the oxygen content of coal feed.[18] It is well-known that particle heating and devolatilization depend on the particle size and heat rate. Using comparable fluid-bed tests, Pillai[19] measured and correlated devolatilization times for a variety of coals, temperatures, and particle sizes. Devolatilization times were estimated to be 1−3 s in the transport reactor using Pillai's empirical correlations. This is well within the residence time of the transport unit. This is also supported by the observation that volatiles are not found in any significant quantity in the downstream experimental equipment.

The combustion kinetics is also assumed to be instantaneous. The combustion reaction produces CO, CO_2, and H_2O. The char combusts with oxygen to yield CO and CO_2 at a molar ratio of unity.[18] Because oxygen is the limiting reactant, the carbon conversion via combustion is simply dependent on the oxygen available.

Gasification. The solids flow pattern in the riser of CFB is complex and difficult to characterize. Therefore, it is assumed on the basis of CSTR studies that solids and gases are well-mixed and that gasification occurs uniformly. The solids temperature is assumed to be equal to the gas temperature. The water−gas shift reaction is assumed to be at equilibrium. The coal, char, and sorbent particles are assumed spherical and of uniform size. The gasification takes place in the presence of CO, CO_2, H_2, H_2O, CH_4, N_2, H_2S, NH_3, char, sorbent, and ash produced from devolatilization and combustion. In this work, a two-parameter model is used to explain the initial and final behavior of char gasification,[18] which is defined by

$$x = 1 - \exp\left(\frac{-KR_o t}{1 + AKR_o t}\right) \quad (11)$$

where K and R_o describe the initial carbon conversion behavior and A describes the final carbon conversion behavior. The parameter x is the carbon conversion. The value of K is the coal-dependent reactivity, which ranges from a value of 50 for lignite to 5 for anthracite. R_o is a function of the pressure, temperature, and gas composition, and it was estimated by Mühlen et al.[20]

$$R_o = \frac{r_1 P_{CO_2} + r_8 P_{CO_2} + r_9 P_{H_2O} + r_{11} P_{H_2O}^2 + r_{12} P_{H_2O} P_{H_2} + r_4 P_{H_2}^2}{1 + r_2 P_{CO_2} + r_3 P_{CO} + r_{10} P_{H_2O} + r_5 P_{H_2}} \quad (12)$$

The rate constant, r_i, was calculated from

$$r_i = k_{o_i} \exp\left(-\frac{E_i}{RT}\right) \quad (13)$$

The values of k_o and E are given by Mühlen et al.[20]

The total average conversion for a CSTR is estimated using

$$X_{avg} = \int_0^\infty \frac{x}{t_{avg}} \exp\left(-\frac{t}{t_{avg}}\right) dt \quad (14)$$

where t_{avg} is the solids average residence time and is obtained from

$$t_{avg} = \frac{I_r}{\mathring{m}_s} \quad (15)$$

The product composition was determined from the elemental balance, the distribution of each element in the gas and solid phases, and the carbon conversion and by adjusting the gas-phase components according to the water−gas shift reaction.

Sulfur Capture. The sulfur released to the gas phase was assumed to be proportional to the converted carbon in the coal and is released as H_2S. The rate of sulfur capture is dependent on whether the partial pressure of CO_2 is above or below that required at equilibrium according to the reaction[18]

$$CaCO_3 \rightleftarrows CaO + CO_2$$

If the CO_2 partial pressure is lower than that required for equilibrium of reaction above, then it was assumed that this reaction occurs completely. In this case, the sulfur capture was obtained according to the reaction

$$CaO + H_2S \rightarrow CaS + H_2O$$

If the CO_2 partial pressure was higher than that required for equilibrium, then the sulfur capture was obtained according to the reaction

$$CaCO_3 + H_2S \rightarrow CaS + CO_2 + H_2O$$

The sulfur capture behavior is estimated by the CSTR model.

Solution Procedure

A mathematical model was developed to describe the gasification of coal in a CFB. The model consisted of 20 nonlinear equations[18] and was developed in MatLab. The inputs to the model were specified as (1) the gas superficial velocity; (2) the solids circulation rate; (3) the reactor pressure and size; (4) the coal and sorbent

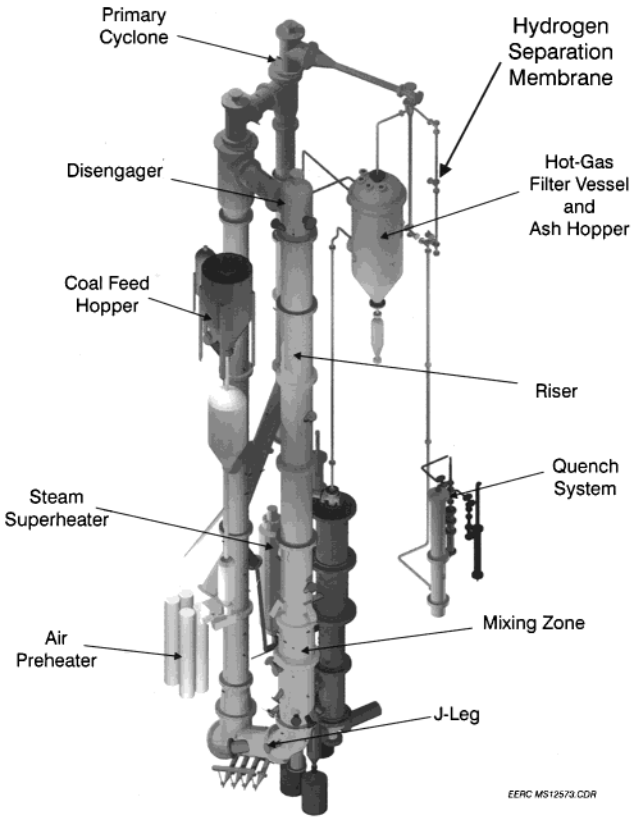

Figure 1. Schematic of the Transport Reactor Development Unit.

flow rates, including the proximate and ultimate analyses of the coal; (5) the steam and purge-gas flow rates; (6) all of the stream temperatures; and (7) the heat lost from the reactor.

The outputs from the model were (1) the product gas flow rates and their compositions, (2) the total carbon conversion, (3) the sulfur capture and sorbent conversion, (4) the reactor temperature, and (5) the air/oxygen required.

The 20 equations were solved simultaneously including (1) the CH_4 and NH_3 balances based on their specified values; (2) the circulation rate; (3) the volatile yield; (4) $CaCO_3$ and $MgCO_3$ dissociation; (5) the ash, Mg, N, S, C, Ca, O, and H balances; (6) the CaO conversion; (7) the shift equilibrium; (8) the energy balance; and (9) the carbon conversion. The calculation procedure was initiated by assuming a set of values for the first 16 variables; the last 4 equations were used to verify the assumed variables. The procedure was iterated using MatLab software routine referred to as the memory model. The nonlinear equations were solved using a quasi-Newton method.

Description of the Experiments

The Transport Reactor Demonstration Unit (TRDU) system can be divided into three sections: the coal feed section, the TRDU, and the product recovery section. The TRDU proper, as shown in Figure 1, consisted of a riser reactor ($h = 12.2$ m, $D_r = 8.9$ cm) with an expanded mixing zone at the bottom ($h = 3.1$ m, $D = 11.4$ cm), a disengager, and a primary cyclone and standpipe ($h = 15.8$ m, $D = 11.4$ cm). The standpipe was connected to the mixing section of the riser by a J-leg transfer line ($h = 2.2$ m, $D = 11.4$ cm). All of the components in the system were refractory-lined and designed mechanically for 1034 kPa (gauge) and an internal temperature of 1090 °C.

The premixed coal and limestone feed to the transport reactor were admitted through one nozzle located near the top of the mixing zone (gasification). The coal feed was measured by a rpm-controlled metering auger. Oxidant was fed to the reactor through two pairs of nozzles at varying elevations within the mixing zone. Hot solids from the standpipe were circulated into the mixing zone, where they mixed with the nitrogen and the steam being injected into the J-leg. This feature ensured that spent char contacted steam before fresh coal feed. This staged gasification process is expected to enhance the process efficiency. The gasification or combustion and desulfurization reactions are thought to be carried out in the riser as coal, sorbent, and oxidant (with steam for gasification) flow up the reactor.

The riser, disengager, standpipe, and cyclones were equipped with several internal and skin thermocouples. Nitrogen-purged pressure taps were also provided to record differential pressures across the riser, the disengager, and the cyclones. The data acquisition and control system scanned the data points every 0.5 s and saved the process data every 30 s. The bulk of the entrained solids leaving the riser was separated from the gas stream in the disengager and circulated back to the riser via the standpipe. A solids stream can be withdrawn from the standpipe via an auger to maintain the system's solids inventory; however, during these steady-state test periods, no solids were continuously removed from the standpipe. Gas exiting the disengager entered a primary cyclone. The solids collected in the primary cyclone, dipleg solids, were recirculated back to the standpipe through the dipleg crossover. Gas exiting this cyclone entered a jacketed-pipe heat exchanger before entering the hot gas filter vessel (HGFV). The cleaned gases leaving the HGFV entered a quench system before being depressurized and vented to a flare. The solids that were not captured by the cyclone were indeed lost to the process, and the carbon in this flyash was counted as unconverted carbon. For example, when the carbon conversion reached 75%, the carbon lost to the downstream equipment represented 25% of the feed carbon.

The quench system used a sieve tower and two direct-contact water scrubbers to act as heat sinks and to remove impurities. All water and organic vapors were condensed in the first scrubber, with the second scrubber capturing entrained material and serving as a backup. The condensed liquid was separated from the gas stream in a cyclone that also served as a reservoir. This liquid was pumped either to a shell-and-tube heat exchanger for reinjection into the scrubber or down to the product receiver barrels.

The coals tested experimentally were Wyodak subbituminous, Illinois #6 bituminous, and Sufco bituminous coals. The results of the proximate and ultimate analyses of these coal are given in Table 1. Experimental tests were conducted on each coal. In each test, the steady-state operating conditions were optimized for product gas quality by adjusting the air and steam feed rates, coal and sorbent feed rates, circulation rate, and superficial gas velocity. The effect of the air and steam flow rate was also tested on the performance of the reactor for the Sufco coal.

Table 1. Proximate and Ultimate Analysis of Coal

	−2 mm Wyodak	−2 mm Illinois No. 6	−2 mm Sufco
proximate analysis, as run, wt %			
moisture	20.0	8.5	9.5
volatile matter	38.9	36.0	39.1
fixed carbon	36.4	44.8	43.8
ash	4.7	10.7	7.6
ultimate analysis, MF wt %			
carbon	69.06	69.27	77.10
hydrogen	5.19	5.03	4.61
nitrogen	0.84	1.1	1.29
sulfur	0.44	3.55	0.36
oxygen	18.63	9.34	8.29
ash	5.85	11.7	8.4
high heating value			
moisture-free, kcal/kg	6505	6716	6783
as-received, kcal/kg	5421	6283	6138

Table 2. TRDU Experimental Conditions and Model Inputs

TRDU test series	PO56	PO57	PO57	PO56
date	2/24/98	4/7/98	4/7/98	2/22/98
	Illinois #6	Sufco#1	Sufco#2	Wyodak
coal feed rate (kg h^{-1})	105.5	99.2	99.2	125.5
coal feed temperature (K)	295	295	295	295
bed pressure (kPa)	927	927	927	927
circulation rate (kg h^{-1})	1638	1832	1832	1923
velocity of product gas (m s^{-1})	7.34	9.5	9.5	7.86
air temperature (K)	422	422	422	422
air flow rate (m^3 h^{-1})[a]	223	279	272.5	275
purge gas rate (m^3 h^{-1})	108.6	136	165	124.6
steam flow rate (m^3 h^{-1})	54.4	54.4	19.3	48.4
steam temperature (K)	573	573	573	573
sorbent feed rate (kg h^{-1})	26.3	5.2	5.2	6.6
sorbent temperature (K)	295	295	295	295

[a] All volume flow rates are at standard conditions.

Table 3. TRDU Experimental Performance Measurements on Gasification Tests

parameter	PO56	PO57	PO56 and PO57
coal	Ill. #6	Sufco	Wyodak
moisture content (%)	8.5	9.5	20.0
pressure (bar)	9.3	9.3	9.3
steam/coal ratio (kg/kg of coal)	0.39	0.14−0.41	0.29
air/coal ratio (kg/kg of coal)	2.59	3.34−3.45	2.69
Ca/S mole ratio (sorbent)	2.0	2.0	2.0
coal feed rate, kg/h	105.5	99.8	125.5
J-leg zone (°C, avg)	901	866−876	800
mixing zone (°C, avg)	935	920−950	850
riser (°C, avg)	923	894−914	840
standpipe (°C, avg)	856	828−860	790
TRDU outlet (°C, avg)	870	856−877	795
carbon conversion (%, solids anal)	76	72−87	89
carbon conversion (%, gas-make)	60	61−64	89
carbon in bed (%, standpipe)	6−15	5−20	6−15
riser velocity (m/s)	7.3	7.6−9.5	9.2
circulation rate (kg/h)	1814	1202−1905	1360−2721
HHV of fuel gas, act. (kcal/m^3)	543	463−668	552−668
cor. (kcal/m^3)	1006	828−1157	935−1042
duration (h)	41	118	179

Results and Discussion

Over 1800 h of operation on the transport reactor in gasification mode have been achieved over the last 4 years. The test campaigns analyzed here included over 300 h of gasification: 179 h on Wyodak subbituminous coal, 41 h on Illinios No. 6 bituminous coal, and 118 h on Sufco bituminous coal. The operating conditions and performance achieved during these tests are summarized in Tables 2 and 3, respectively. The TRDU was operated at an average temperature of 875 °C for the Wyodak coal tests and up to 950 °C for the bituminous coal tests. Coal feed rates ranged from 100 up to 150 kg/h depending on the coal type and operating conditions, and the gasifier pressure averaged 830 kPa. The raw moisture-free product gas produced ranged from 6 to 10% CO and H_2, from 9 to 11% CO_2, and from 1.0 to 2.5% CH_4, with the balance being N_2 and other trace constituents. These were the first tests to recirculate dipleg solids back into the standpipe and also the first tests to inject air into the J-leg nozzles. These changes allowed the TRDU to better utilize the fine char and sorbent material that carried over to the primary cyclone and also to operate at lower riser velocities for increased residence time. The H_2S concentration averaged 50 ppm for the low-sulfur fuels and 400 ppm for the high-sulfur Illinois No. 6 coal. Correction of the fuel gas concentrations for the nitrogen purges and the high system heat loss (estimated at approximately 77 000 kcal/h) as a percentage of the coal feed demonstrates that heating values ranging between 830 and 1160 kcal/m^3 can be achieved under air-blown operation.

Factors that affected the TRDU product gas quality appeared to be circulation rate, coal type, temperature, and air/coal and steam/coal ratios. A decrease in the circulation rate improved the product gas quality by increasing the solids residence time in the gasification zones of the TRDU; however, experience has shown that lower-circulation-rate tests are more prone to deposition and agglomeration problems as a result of inadequate gas−solid mixing in the mixing zone. The less-reactive bituminous fuels were gasified at higher temperatures to produce a product gas quality similar to that obtained with the Wyodak fuel. Higher operating temperatures increased carbon conversion for the TRDU but again at the risk of increased ash deposition. Higher steam/coal ratios resulted in improved product gas quality with increased hydrogen and carbon dioxide formation from the water−gas shift reaction, but additional CO was also produced. Higher air/coal ratios gave lower product gas quality, especially at ratios above 3.5. The best product gas was generally observed when the air/coal ratio was under 3.0.

The model predictions were compared to the experimental results taken under these experimental operating conditions (Table 4). These validation simulations were conducted by setting the flows, the coal reactivity, and the feed conditions and adjusting the heat loss. Heat losses from the transport reactor were varied within the experimental range (estimated to be between 75 000 and 100 000 kcal/h) in order to best match the temperature and air flow rate. This amounts to approximately 20% of the heating value for the feed coal. The recycle temperature was assumed to be 55.6 K below the reactor temperature. Performance measurements included the gas composition, carbon conversion, and temperature. The carbon conversion used for these comparisons was based on the gas analysis (gas-make) because gas samples were systematically taken using standard and accurate measurements methods. This approach also avoids the inaccuracies of the slowly changing composition of the solids between steady-state periods and the difficulties of obtaining representative solids samples and measuring the solids flow rates.

In general, the average standard error between the model and the experimental values was 5.8%. Moreover, 19 of the 32 parameters agreed to within 5%, and 29 parameters agreed to within 10%. The largest errors for these test cases were in the CO yields, which were

Table 4. Comparison between the Model and TRDU Experiment

	Illinois #6		Sufco#1		Sufco#2		Wyodak	
	exp	model	exp	model	exp	model	exp	model
CO (vol. %, dry basis)	6.6	7.5	6.7	7.45	7.0	9.0	7.8	9.0
H_2	7.9	8.5	6.5	7.0	5.2	5.4	8.4	9.4
CO_2	11.6	10.5	10.2	10.2	8.6	8.0	11.5	11.3
CH_4	1.5	1.64	1.8	1.76	1.6	1.6	1.7	1.7
N_2	73.7	71.5	74.0	73.3	77.0	75.8	71.2	68.5
HHV (kcal/m^3)	552	552	542	536	498	555	640	645
carbon conv. (wt %)	60.3	54.5	61.6	68.7	64	67.6	88.5	85.3
temperature (K)	1227	1227	1205	1200	1205	1222	1133	1136

between 13 and 29% too high in the simulations. This discrepancy might be an indication that the assumed CO/CO_2 ratio of unity during combustion was somewhat high. Measurements of CO/CO_2 are reported to depend on temperature.[21] It is expected that the nature of the carbon char and the presence of catalytic species on the surface might also affect this combustion pathway. Froehlich et al.[22] evaluated different temperature-dependent $CO/(CO+CO_2)$ ratios for each coal studied in a spouted fluid-bed carbonizer. Linjewile and Agarwal[23] reported values of 0.1−0.5 for fluidized-bed combustion of petroleum coke spheres that were independent of temperature over the range of conditions studied. Further research is needed, particularly at the shorter residence times used in transport reactors.

The Wyodak simulations were the most difficult to match with the experimental data. Initially, 3 of the 8 modeled values, including the carbon conversion and gas heating value, differed by more than 20% from the test data. Attempts to match the conversion by adjusting the reactivity within the reported literature range and observed heat losses were not successful in achieving carbon conversion levels above 70%. However, when the reactivity factor, K, was increased by a factor of about 20 up to a value of 1000, all of the parameters agreed within a 15% standard error.

The high-reactivity Wyodak case provided the only test case in which the carbon conversion from gasification was greater than 3 or 4%. Thus, it is the only case in which the gasification reactivity parameters can be validated with any accuracy. The other experimental cases were fit accurately, but because gasification was insignificant, it is impossible to extrapolate those coals to conditions that might exhibit significant gasification. The mass and energy balances for these coals using only combustion reactions were sufficient to explain the test data. The finding that the model accurately predicted conversion, temperature, and gas composition for Wyodak coal under gasification provided a calibration point of the model's sensitivity to this coal's reactivity.

The effects of steam flow rate on product gas composition and carbon conversion are illustrated in Table 4 for the Sufco coal in a substoichiometric combustion regime. At low steam flow rate (Sufco#2), the percentage of CO is higher than that of H_2 (7.0% compared to 5.2%) in the product gas. As the steam flow rate was increased (Sufco#1), the percentage of CO decreased, and that of H_2 increased. The observed functional dependence arose from the fact that the water−gas shift reaction is more favorable for the production of H_2 at higher steam flow rates. Also, the higher steam flow rate resulted in increased heating values (Table 4). This is because the temperature for both cases (high and low steam flow rates) was maintained constant at 1205 K.

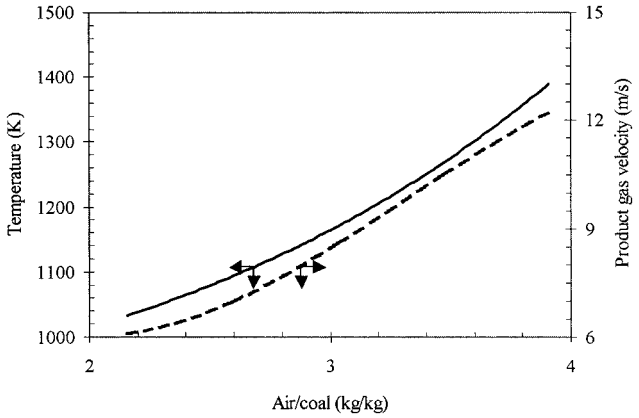

Figure 2. Simulation of the Wyodak coal case predicting the influence of the air/coal ratio on the temperature (—) and product gas velocity (− − −).

Parametric Analysis

Model simulations were computed at different values of various operating conditions, including coal flow rate, steam/coal ratio, heat loss, gas velocity, and system pressure. The gasifier performance parameters of interest were the carbon conversion, temperature, gas composition, and fuel gas heating value. Each process parameter was varied independently, while the others were held constant. The conditions used in the base case for the parametric study are the same as the TRDU experimental conditions presented in Table 2. This study was first conducted using the properties and conditions for the Illinois #6 bituminous coal and was then repeated using the Wyodak coal properties. In this way, the response of the reactor operating under a process is dominated by partial combustion can be compared to the response of a process with significant contribution from char gasification.

The most important operating factor in a coal gasifier is the air/coal ratio as it determines the reaction temperature. The impact of the air/coal ratio was determined for the Wyodak coal case (Figures 2−4) by varying the air flow for a constant coal feed rate and allowing the product gas velocity to increase. The temperature increased from 1040 to 1400 K over the tested air/coal ratio (Figure 2), indicating a greater contribution from the exothermic combustion processes. The carbon conversion was very sensitive to this temperature increase (Figure 3). At low air/coal ratios, the carbon conversion increased as a combined result of both combustion and gasification reactions. At air/coal ratios above 3, the carbon conversion was nearly complete. At higher air/coal ratios (>3), combustion reactions consumed more of the char, thereby making it unavailable for gasification conversion.

This was also reflected in the gas composition (Figure 4). As the air/coal ratio was increased from 2 to 3, the

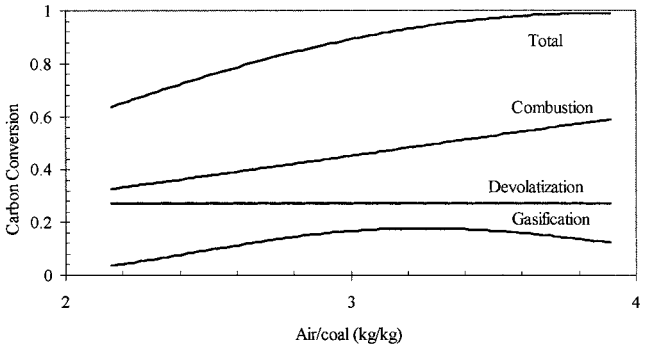

Figure 3. Simulation of the Wyodak coal case predicting the influence of the air/coal ratio on the carbon conversion via combustion, gasification, and devolatilization processes.

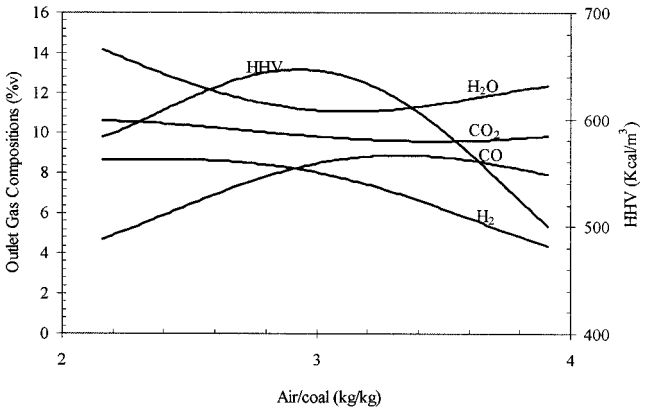

Figure 4. Simulation of the Wyodak coal case predicting the influence of the air/coal ratio on the product gas heating value and composition including H_2, CO, CO_2, and H_2O.

water content in the product gas decreased, and the carbon monoxide content increased, resulting in an overall increase in the calorific value of the product gas. These improvements to the gas composition can be traced to an increased utilization of steam and carbon dioxide via gasification reactions. Above an air/coal ratio of 3, combustion reactions dominated: less steam was converted to H_2 via the carbon−steam reaction, and less CO_2 was converted to CO via the CO_2−char reaction. The result was higher CO_2 and H_2O contents in the product gas and less H_2 and CO and an overall reduction in the product gas heating value. These results indicate that reactor performance is optimized at an intermediate air/coal ratio of about 3.

The overall effect of product gas velocity on all dependent parameters was small. The solids residence time decreased from 18.3 to 15 s over the range of air/coal ratios tested, but apparently this had little resulting impact on the coal conversion behavior. Simulations conducted by changing the gas velocity while holding the air/coal ratio constant over this range of flows indicated only a very slight impact on temperature or conversion.

The heat loss from the transport reactor will be substantially reduced as the process is scaled up to a commercial-sized unit. The impact of heat loss was examined using a constant coal feed and air/coal ratio, as presented in Figures 5−7. The transport reactor ran with about 20% heat loss relative to the nominal coal feed rate. The model predicts that conversion approaches completion at heat losses below 10% (Figure 5). Heat losses above 10% reduced carbon conversion solely because of the gasification reactions. Combustion

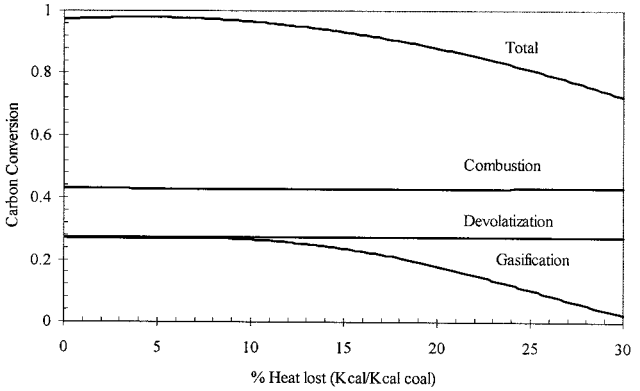

Figure 5. Simulation of the Wyodak coal case predicting the influence of heat loss on the carbon conversion via combustion, gasification, and devolatilization processes.

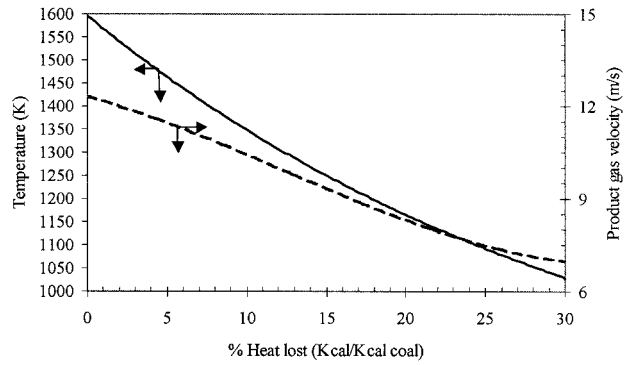

Figure 6. Simulation of the Wyodak coal case predicting the influence of heat loss on the temperature (—) and product gas velocity (− − −).

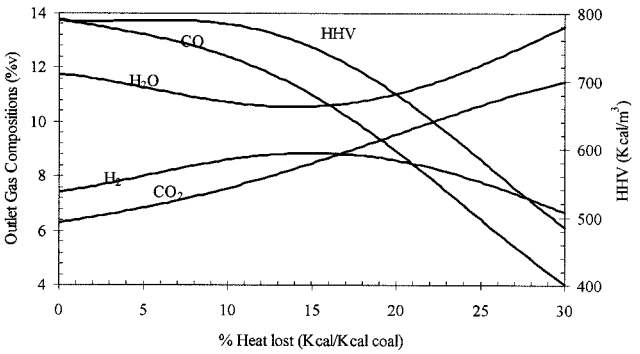

Figure 7. Simulation of the Wyodak coal case predicting the influence of heat loss on the product gas heating value and composition including H_2, CO, CO_2, and H_2O.

conversion was unaffected because the air/coal ratio was kept constant for these simulations. The reactor temperature dropped nearly linearly from 1600 K (0% heat loss) to 1050 K (25% heat loss) (Figure 6). As a result of the drop in temperature, the product gas velocity decreased. The decrease in gas velocity caused only a slight increase in residence time, because the circulation rate was low and the reactor was being operated in a dilute-phase transport regime. Predicted changes in the gas composition and calorific value due to variations in heat loss are shown in Figure 7. As the heat loss increased, the percentage of carbon dioxide in the product gas increased, while the percentage of CO decreased. This is consistent with experimental data reported by Perry et al.[24] Below 10% heat loss, the H_2 content in the gas increased and reached a plateau. Above 15% heat loss, the temperature dropped enough

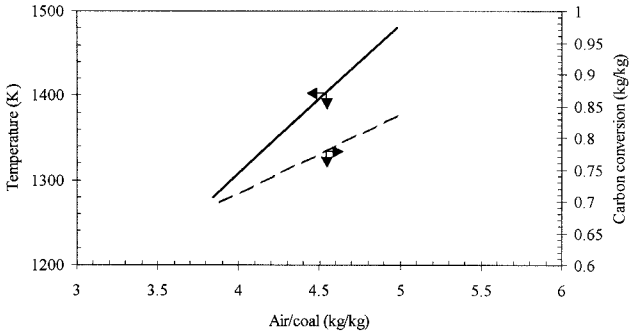

Figure 8. Simulation of Illinois #6 coal predicting the influence of air/coal ratio on the temperature (—) and carbon conversion (– – –).

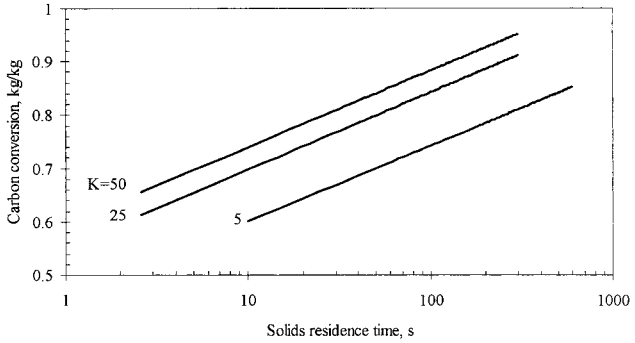

Figure 9. Predicted influence of the coal reactivity factor, *K*, on the carbon conversion via gasification using test conditions for the Illinois #6 test case at 1311 K and varying solids residence times.

to slow the carbon steam reaction; this increased the H_2O content and decreased the H_2 levels. These results suggest that the minimization of heat loss is desirable and that the greatest gain can be obtained by reducing heat losses to below 10% of the coal feed heating value.

The coal feed rate was varied while a constant air/coal ratio was maintained. The coal feed rate increased the temperature very slightly (from 1080 to 1150 K for a change from 70 to 160 kg/h feed rates). There was almost no impact on carbon conversion, although 3−4% additional conversion was achieved from gasification. This additional conversion was accompanied by slightly higher CO and H_2 and lower CO_2 and H_2O yields, resulting in higher heating values (increase from 570 to 660 kcal/m^3). This suggests that performance improves slightly as the feed rate increases.

There were only slight decreases in carbon conversion, temperature, and gas product heating value as the steam/coal ratio increased over the range of 0.20−0.50. Steam was not a limiting reactant over these operating conditions. The increased moisture contents in the product gas served to dilute the gas and reduce the heating value of the fuel gas. The water−gas shift equilibrium predicted that the CO concentration would drop as the moisture levels increased. No significant change was noted for CO_2 and H_2.

The circulation rate was varied from about 1900 to 6300 kg/h while the air-to-coal ratio was kept constant. If the char recycle temperature was equivalent to the bed temperature, then there was no impact of circulation rate on conversion or temperature. However, if the recycle char temperature was lowered in the recycle loop, then the temperature in the gasifier decreased proportionately. Thus, the impact of the circulation rate depended mainly on heat losses in the downcomer of the transport reactor; large heat losses in the downcomer can hurt performance, but negligible heat losses do not improve reaction chemistry performance over the range of solids residence times achieved (2−8 s). The impact of the circulation rate can be thought to be on the solids mixing and solids residence times, as discussed below.

A sensitivity study was also performed on a nonreactive coal. When the coal type is nonreactive, gasification reactions do not contribute to carbon conversion. In this case, the response to process operating variables differs from that observed in the Wyodak coal case presented above. An analysis of the Illinois #6 coal using literature kinetic rate constants[20] indicates this type of behavior (Figure 8). This sensitivity analysis was conducted by varying the coal feed rate. The air/coal ratio was substantially higher than that needed for the Wyodak coal. The temperature increase for each unit change in air/coal ratio was much higher for the Illinois #6 coal, because endothermic carbon−steam and carbon−CO_2 reactions did not contribute. The increase in carbon conversion per unit change in air/coal ratio, on the other hand, was much lower than for the Wyodak case. Temperatures became exceedingly high (1480 K) without the accompanying increases in carbon conversion. The reactor was unproductive in this situation.

The effect of coal type on carbon conversion was evaluated by varying the reactivity factor, *K*, from eq 11. The influence of reactivity is presented in Figure 9 for a reactor temperature of 1310 K using the Illinois #6 test conditions over a range of solids residence times. Because the reactivity factor is in the exponential term, its effect on carbon conversion is larger at lower reactivities and becomes incrementally smaller for more-reactive coals. The effect of the solids residence time is also exponential, requiring a logarithmic time scale. The extent of carbon conversion was predicted to be 60−75% over the range of recommended reactivity factors (K = 5−50). This model predicted that 30−100-s residence times were required to obtain greater than 80% carbon conversion for coals with these reactivities. However, when the fitted reactivity for the Wyodak coal was used (K = 500−1000), the carbon conversion levels exceeded 85% within the 15-s residence time available in the transport reactor.

To match the simulation results with the test data from the Wyodak coal, a reactivity of *K* equal to 500−1000 was required. Although this value represents an increase of 20 times over the kinetic parameters suggested,[18] the direction and magnitude of this difference are not unexpected for a process such as that occurring in the transport reactor. First, one must consider the fact that variations of a factor of 5−10 are observed for low-rank coals of the same carbon content.[5,25] This variability can be understood when taken in the context of studies on the catalytic species in low-rank coals. In low-rank coals, the presence of catalytic species dispersed throughout the organic matrix leads to a factor of 2−3 times increase in reactivity.[26] Heating such coals to 1275 K for as short as 30 s produces significant CaO crystallite growth and a 10-fold drop in reactivity.[9]

In addition, the kinetic expressions and associated constants initially applied in this model were developed for chars generated under high heating rates but then cooled and heated back to operating temperature before the gasification rates were measured.[20] Such temperature cycling is known to deactivate the char.[27,28] This is thought to occur through processes similar to anneal-

ing of the char surface[5,7] and, for low-rank coals, loss in dispersion of catalytic species on the surface. Thus, these studies can be thought to provide a lower bound to the reactivity in high-heating-rate processes such as those occurring in the transport reactor.

Within the transport reactor, the coal is injected into a high-velocity, high-temperature flow stream. The air is introduced into a lower region of the bed, well below the coal, and the oxygen is likely consumed by the hot recycled char. This spatial separation is designed to minimize the exposure of the coal and volatiles to oxygen, thereby reducing the generation of high local temperatures on the surface of the char. For the Wyodak coal, the temperatures are quite low, 1125 K, and the solids residence time is estimated to be about 15 s. As such, the time and temperature required for devolatilization, and thus the time available for morphological changes to occur in the char and mineral structure, is minimized. At the same time, the high relative velocity between the gas and solids results in rapid diffusion of gasification reactants into the open-pore structure produced by the high heating rates. All of these factors tend to enhance the observed reactivity relative to the values reported in the literature.

The overall riser slip factors were estimated to be between 2 and 10. The overall riser slip factor was determined from the measured circulation rate (as determined from an incremental pressure drop along the top of the riser) divided by the gas velocity. Because of the wider section in the mixing zone, the gas velocity there is lower, and the resulting slip is higher. Averaged over the entire length of the riser, the slip was calculated to approach 10 for some cases.

Fluidization Regimes in TRDU

According to this model, the operating parameters most critical to conversion, besides coal type, are residence time and temperatures. Operating parameters such as the coal particle size, the gas velocity, the reactor diameter, and the solids circulation rate have no effect on the validated mechanisms described above, but they do impact the solids residence time. If the reactor continues to operate in the dilute regime, the residence time can only be affected marginally, i.e., over the range of 2−10 s. However, a change of flow regime can significantly increase the residence times.

The solids residence time for a transport reactor depends on its geometric and operational parameters. Residence times are on the order of 2−30 s for a reactor like the TRDU, i.e., with a 16.5-m height and a 8.9-cm inner diameter. Such values can be directly calculated from the pressure drop and height and circulation rate using eq 15. Experimental measurements indicate that 10−15-s solids residence times were obtained during these coal tests. The transport reactor was operated in the dilute transport regime. According to the correlations developed by Bi and Grace[29] and recently verified for 230-μm sized coke particles in a 30.48-cm-diameter and 14.78-m-high CFB at NETL, increasing the circulation rate from 200 to 500 g/s (or from 0.024 to 0.058 cm/s) would move the riser into the core-annular flow regime (Figure 10). Maintaining the same gas flows, the mixing zone is projected to become fast-fluidized when the circulation rate approaches 750 g/s. Adverse characteristics of a fast-fluidized bed includes some moderate dynamic instabilities because the dense regions of the bed become filled as the inventory or circulation rate

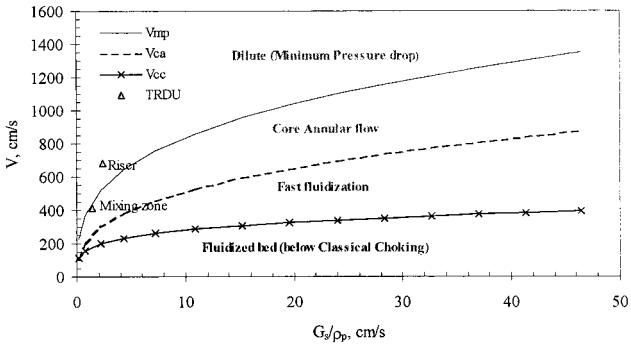

Figure 10. TRDU flow regime map as estimated from Bi and Grace[29] using Illinois # 6 test conditions and resulting solid and gas flow rates, $d_p = 175\ \mu$m, and $\rho_s = 1.4$ g/cm^3. V_{mp} is the velocity limit for minimum ΔP, V_{ca} is the velocity limit for core-annular flow, and V_{cc} is the velocity limit for classical choking.

increases. The advantage of moving from dilute transport to core-annular flow or even further into the fast-fluidized regime is the potential to increase the slip factor and, thus, the solids residence time. Increases by a factor of 5−10 times were observed over these transitions from the dilute regime to the core-annular and fast-fluidization regime.

As operated for these tests, the riser was characterized as homogeneous and dilute, i.e., above the point of minimum pressure drop (Figure 10). However, because of the expanded diameter in the mixing zone at the bottom of the transport reactor, the mixing zone was in the core-annular flow regime. Both of these conditions were true for solids densities of 1.4−2 g/cm^3, simulating significant start-up sand in the bed, and for particle sizes from 175 up to 300 μm. The solids circulation rate and the gas velocity are the most sensitive factors that can practically be varied to improve residence time. At a gas velocity of 700 cm/s, the riser will achieve core-annular flow above 500 g/s; fast fluidization occurs above 1900 g/s. At the same corresponding gas flows, the circulation rate must exceed 7500 g/s to choke in the mixing zone. However, increasing the mixing zone from 11.4 to 14 cm requires only 1900 g/s to drop below the classical choking velocity. In these estimates, it is clear that the riser does not provide an operating constraint; all anticipated future operations occur well above its classical choking velocity, V_{cc}.

Conclusion

A mathematical simulation of CFB coal transport gasifier was developed using the CSTR model for both gasification and sulfur sorption kinetics. Coal conversion was the summation of conversion due to devolatilization, combustion, and gasification processes. The reaction chemistry also included instantaneous coal devolatilization and combustion. Sulfur capture was predicted using in-bed calcium-based sorbents, with the pathway depending on the carbon dioxide partial pressure. Product stoichiometry was dependent on coal composition. Equilibrium of the water−gas shift reaction was used to determine the gaseous product distribution. Hydrodynamic analysis of the gas−solid transport process was used to determine the solids residence time. Although using a CSTR kinetic model can lead to inaccuracies when reactions approach complete conversion, the carbon conversions measured in the TRDU experiment were below 98%. The CSTR approach was found to be quite appropriate for this application.

The model predictions were validated against experimental data and were generally within 10% agreement. The average deviation from the measured values was about 6%. In its present form, the model can be used to provide quantitative insight into the influence of the different parameters on the process performance such as gas composition, temperature, product calorific value, and carbon conversion. The methane yield was specified as a model input that describes the devolatilization product stoichiometry. A value of unity was used for the CO/CO_2 ratio produced during char combustion. Predictions of the carbon conversion and product distribution will be affected by the expression used for this ratio.

A sensitivity analysis was performed on the key parameters such as coal type, coal feed rate, air and steam flow rates, heat lost, solids circulation rates, and gasifier pressure. Coal type was the single most important parameter. The reactive Wyodak coal was found to have a conversion rate significantly greater than recommended values. This is thought to be due to the nature of the process conditions in the TRDU, which avoid annealing and sintering of catalytic species on the coal surface. No such apparent enhancements in the reactivity were observed for the bituminous coals used in this process. The behavior of these lower-reactivity coals was dominated by the partial combustion process. Conversion was directly related to the air/coal ratio, and the temperature increased directly with these combustion reactions.

For the reactive low-rank coal, the behavior was influenced by those parameters that most affected temperature. The air-to-coal ratio was the most important operating parameter affecting temperature. Carbon conversion was very sensitive to operating temperature. Carbon conversion reached completion near an air-to-coal ratio of 3; above that value, the product gas quality was adversely impacted. The heat loss also directly affected reaction temperature, with losses of less than 10% required to approach complete conversion. Variations in the steam-to-coal ratio affected temperature primarily by affecting the sensible heat requirements. Steam concentrations required for gasification were generally small relative to the steam formed upon combustion and released from the coal, and so, they did not have any impact on the gasification rates.

When the air-to-coal ratio was fixed at a constant value, the following operating parameters exhibited little or no impact on conversion and gas product composition: coal feed rate, solids circulation rate, gas velocity, and gas pressure. In this manner, all of these factors tested various aspects of varying the residence time in the reactor, admittedly over a relatively small time window between 2 and 30 s. There was a small effect on the gasification conversion (3−4%) when the effect of the coal feed rate was tested, indicating the low magnitude of the time dependence over this operating window.

Acknowledgment

The authors acknowledge the Department of Energy for funding the research through the Fossil Energy's Integrated Gasification Combined-Cycle program.

Nomenclature

A_r = cross-sectional area of the riser (m^2)
a = decay constant (m^{-1})
D_r = riser diameter (m)
E_i = activation energy for reaction i (kJ mol^{-1})
g = gravitational constant (m s^{-2})
G_s = solids circulation flux (kg m^{-2} s^{-1})
h = axial height (m)
H_{dense} = height of dense region (m)
H_{dil} = height of dilute region (m)
I_{dense} = solids inventory in the dense region (kg)
I_{dil} = solids inventory in the dilute region (kg)
I_r = solids inventory in the riser (kg)
L_r = length of the riser (m)
$\mathring{m}_s$ = solids circulation rate (kg s^{-1})
P = pressure (bar)
T = temperature (°K)
t_{avg} = average solids residence time (s)
r_i = rate constant for rection i
R_o = gasification reaction rate (s^{-1})
t = time (s)
U_g = superficial gas velocity (m s^{-1})
U_t = terminal velocity (m s^{-1})
x = carbon conversion
X_{avg} = average carbon conversion

Greek Letters

ϵ^* = voidage above TDH
$\bar{\epsilon}_{dense}$ = average voidage in the dense region
$\bar{\epsilon}_{dil}$ = average voidage in the dilute region
ϵ_e = riser exit voidage

Literature Cited

(1) Longanbach, J.; Moorehead, E.; Styles, G.; Vimalchand, P. Transport Reactor Development Gives a Boost to U.S. Coal-Fired Plant. *Mod. Power Syst.* **1996**, *Nov.*, 37.

(2) Anthony, D. B.; Howard, J. B. Coal Devolatilization and Hydrogasification. *AIChE J.* **1976**, *22* (4), 625.

(3) Solomon, P. R.; Serio, M. A.; Suuberg, E. M. Coal Pyrolysis Experiments, Kinetic Rates, and Mechanisms. *Prog. Energy Combust. Sci.* **1992**, *18*, 133.

(4) Essenhigh, R. H. Fundamentals in Coal Combustion. In *Chemistry of Coal Utilization*; Elliot, M. A., Ed.; John Wiley & Sons: New York, 1981; Second Supplementary Volume, p 1153.

(5) Jenkins, R. G.; Nandi, S. P.; Walker, P. L., Jr. Reactivity of Heat-Treated Coals in Air. *Fuel* **1973**, *52* (10), 288.

(6) Molina, A.; Mondragón, F. Reactivity of Coal Gasification with Steam and CO_2. *Fuel* **1998**, *77*, 1831.

(7) Blake, J. H.; Bopp, G. R.; Jones, J. F.; Miller, M. G.; Tambo, W. Aspects of the Reactivity of Porous Carbons with Carbon Dioxide. *Fuel* **1967**, *46*, 115.

(8) Nsakala, N. Y.; Essenhigh, R. H.; Walker, P. L., Jr. Characteristics of Chars Produced from Lignites by Pyrolysis at 808 °C Following Rapid Heating. *Fuel* **1978**, *57*, 605.

(9) Radovic, L. R.; Walker, P. L., Jr.; Jenkins, R. G. Importance of Catalyst Dispersion in the Gasification of Lignite Chars. *J. Catal.* **1983**, *82*, 382.

(10) Weiss, V.; Fett, F. N.; Helmrich, H.; Janssen, K. Mathematical Modeling of Circulating Fluidized Bed Reactors by Reference to a Solid Decomposition Reaction and Coal Combustion. *Chem. Eng. Prog.* **1987**, *22*, 79.

(11) Rajan, R. R.; Wen, C. Y. A Comprehensive Model for Fluidized Bed Combustors. *AIChE J.* **1980**, *26*, 642.

(12) Arena, U.; Malandrino, A.; Massimilla, L. Modeling of Circulating Fluidized Bed Combustion of a Char. *Can. J. Chem. Eng.* **1991**, *69*, 860.

(13) Adánez, J.; de Diego, L. F.; Gayán, P.; Armesto, L.; Cabanillas, A. A Model for Predicting Carbon Combustion Efficiency in Circulating Fluidized Bed Combustors. *Fuel* **1995**, *74*(7), 1049.

(14) Yerushalmi, J.; Cankurt, N. T. Further Studies of the Regimes of Fluidization. *Powder Technol.* **1979**, *24*, 187.

(15) King, D. F. Estimation of Dense Bed Voidage in Fast and Slow Fluidized Beds of FCC Catalyst. In *Fluidization VI*; Grace, J. R., Shemilt, L. W., Bergougnou, M. A., Eds.; New York, 1989; p 1.

(16) Kunii, D.; Levenspiel, O. Entrainment of Solids from Fluidized Beds I. Hold-Up of Solids in the Freeboard II. Operation of Fast Fluidized Beds. *Powder Technol.* **1990**, *61*, 193.

(17) Wen, C. Y.; Chen, L. H. Fluidized Bed Freeboard Phenomena: Entrainment and Elutriation. *AIChE J.* **1982**, *28*, 117.

(18) Shinnar, R.; Rinard, I.; Avidan, A.; Weng, L.; Eng, A. *Gasification of Coal Process Modeling Simulation*; Department of Chemical Engineering, The City College of New York: New York, 1990.

(19) Pillai, K. K. The Influence of Coal Type on Devolatilization and Combustion in a Fluidized Bed. *J. Inst. Energy* **1981**, 142.

(20) Mühlen, H.-J.; van Heek, K. H.; Jüntgen, H. Kinetics Studies of Steam Gasification of Char in the Presence of H_2, CO_2, and CO. *Fuel* **1985**, *64*, 944.

(21) Arthur, J. R. Reaction Between Carbon and Oxygen. *Trans. Faraday Soc.* **1951**, *47*, 164.

(22) Froehlich, R.; Robertson, A.; VanHook, J.; Goyal, A.; Rehmat, A.; Newby, R. *Second-Generation Pressurized Fluidized Bed Combustion Research and Development, Phase 2, Task 4 Carbonizer Testing*; DOE Contract DE-AC21-86MC21023; U.S. Department of Energy, U.S. Government Printing Office: Washington, D.C., 1994; p 174.

(23) Linjewile, T. M.; Agarwal, P. K. The Product CO/CO_2 Ratio from Petroleum Coke Spheres in Fluidized Bed Combustion. *Fuel* **1995**, *74* (1), 5.

(24) Perry, H.; Corey, R. C.; Elliott, M. A. Continuous Gasification of Pulverized Coal with Oxygen and Steam by the Vortex Principle. *Trans. ASME* **1950**, *72*, 599.

(25) Miura, K.; Hashimoto, K.; Silverston, P. L. Factors Affecting the Reactivity of Coal Chars during Gasification, and Indices Representing Reactivity. *Fuel* **1989**, *68*, 1461.

(26) Hippo, E. J.; Jenkins, R. G.; Walker, P. L., Jr. Enhancement of Lignite Char Reactivity to Steam by Cation Addition. *Fuel* **1979**, *58*, 338.

(27) Agarwal, A. K.; Sears, J. T. Coal Char Reaction with CO_2−CO Gas Mixture. *Ind. Eng. Chem. Process Des. Dev.* **1980**, *19*, 364.

(28) Tamhankar, S. S.; Sears, J. T.; Wen, C. Y. Rates of Coal Gasification at High Temperatures in Carbon Dioxide and Steam. *Proc. Jt. Meet. Chem. Eng., Chem. Ind. Eng. Soc. China Am. Inst. Chem. Eng.* **1982**, *2*, 596.

(29) Bi, H. T.; Grace, J. R. Flow Regime Diagrams for Gas−solid Fluidization and Upward Transport. *Int. J. Multiphase Flow* **1995**, *21* (6), 1229.

Received for review December 18, 2000
Revised manuscript received April 3, 2001
Accepted April 9, 2001

IE001113U